Double-Layer Metamaterial Microwave Sensor for Olive Oil Quality

Fatiha Babaghayou[1,3], Djalal Eddine Bensafieddine[2], Meriam Imane Babaghayou[1], and Tahar Seghier[3]

[1]Laboratoire des Sciences Chimiques et Physiques Appliquées Higher Normal School of Laghouat, Algeria
[2]Department of Physics, Higher Normal School of Laghouat, Laghouat 03000, Algeria
[3]Laboratoire d'Etude et de Développement des Matériaux Semi-conducteurs et Diélectriques Faculté de Technologie, Université Amar Telidjii - Laghouat, Algeria

Corresponding author: Fatiha Babaghayou (e-mail: f.babaghayou@lagh-univ.dz)

ABSTRACT This paper presents a double-layer metamaterial microwave sensor for the selective detection of water adulteration in virgin olive oil. The proposed design employs an E-comb resonator configuration that enhances electric-field confinement and improves interaction between the resonator and the material under test compared with conventional single-layer resonant sensors. The sensor was first characterized through broadband full-wave electromagnetic simulations using CST and HFSS over the 1–15 GHz frequency range, followed by fabrication and experimental validation using vector network analyzer (VNA) measurements. Experimental results demonstrate a strong and selective response to polar contaminants, exhibiting a resonance frequency shift of approximately 0.5 GHz for only 5 % (v/v) water adulteration. In contrast, non-polar adulterants such as sunflower oil produce negligible resonance variation. The dielectric properties of the samples were extracted using the Cole–Cole relaxation model and showed good agreement with reported literature values, confirming the reliability of the proposed sensing mechanism. Furthermore, a quality factor-based index is introduced as a quantitative indicator for assessing oil purity. The proposed approach provides a non-destructive, real-time sensing technique with strong potential for automated quality control in the olive oil industry, using a compact and cost-effective microwave sensing platform.

INDEX TERMS Metamaterials; Microwave sensor; Dielectric properties; Olive oil quality; Vector network analyzer; Quality factor index.

I. INTRODUCTION

Virgin olive oil is widely recognized for its distinctive flavor, nutritional value, and high content of natural antioxidants [1,2]. Due to its high commercial value and increasing consumer demand, however, olive oil is frequently subject to adulteration practices that compromise its authenticity, nutritional quality, and market reliability [3–5]. Among potential contaminants, the presence of water is particularly problematic because it accelerates oxidative degradation, reduces shelf life, and alters the physicochemical stability of the oil. Reliable detection of such adulteration is therefore essential for ensuring product quality and consumer protection.

Conventional analytical methods used for olive oil quality control, including chromatography and spectroscopy techniques [4], provide reliable compositional analysis but often require sophisticated laboratory equipment, trained personnel, and time-consuming sample preparation procedures. Moreover, these techniques are generally destructive and not well suited for rapid in-line monitoring during industrial processing. For these reasons, the development of rapid, non-destructive, and cost-effective sensing techniques for food quality monitoring has become an important research topic [6–8].

In recent years, microwave dielectric sensing and metamaterial-based resonant structures have emerged as promising solutions for non-destructive material characterization and food quality monitoring [2,3,9]. These techniques exploit the strong dependence of the dielectric properties of materials on their chemical composition. In particular, the presence of water significantly alters the dielectric properties of olive oil due to the large difference in dielectric permittivity between water and oil [10,11]. Several studies have investigated dielectric variations in edible oils caused by temperature [1], composition changes [3], or electrical properties measured at low frequencies (e.g., 20 Hz–2 MHz) [12]. However, the use of metamaterial-inspired microwave sensors for detecting water adulteration in olive oil remains relatively limited, despite their demonstrated effectiveness in applications such as biomedical sensing and food quality assessment [13].

Metamaterial resonators, including split-ring resonators (SRRs) and related structures, are particularly attractive for sensing applications because they provide strong electric-field localization in the capacitive regions of the resonator. This field confinement enhances the interaction between the

electromagnetic field and the material under test, allowing small variations in dielectric permittivity to be detected through shifts in resonance frequency and quality factor [13–19]. Nevertheless, conventional planar resonators often provide limited sensing volume and relatively weak interaction with liquid samples, which can restrict sensitivity and detection capability. Consequently, improving electric-field localization and increasing the effective capacitive sensing region remain important design strategies for enhancing microwave sensor performance.

To address these limitations, this study proposes a double-layer metamaterial microwave sensor based on an E-comb resonator geometry for the detection of water adulteration in virgin olive oil. The comb-type structure introduces multiple capacitive gaps that enhance electric-field localization and increase the interaction between the resonator and the liquid sample. In addition, the double-layer configuration improves electromagnetic field confinement in the sensing region, which contributes to improved sensing performance compared with conventional single-layer resonators.

The sensor design and performance were evaluated through a comprehensive methodology. First, the metamaterial unit cell was characterized using CST simulations to confirm its wideband electromagnetic response and effective medium behavior, including negative refractive index characteristics derived from its effective permittivity and permeability parameters [20]. The sensing mechanism was further investigated by analyzing electric-field distribution and current density at resonance, and an equivalent circuit model was developed to provide a physical interpretation of the resonant behavior. The complete sensor structure was then simulated and cross-validated using both CST and HFSS electromagnetic solvers. Subsequently, the sensor was fabricated and experimentally characterized using a vector network analyzer (VNA).

To evaluate the sensing capability, a comparative analysis was performed using three samples: pure olive oil, olive oil adulterated with 5 % (v/v) water, and olive oil mixed with 5 % (v/v) sunflower oil. The dielectric properties of the samples were extracted from the measured scattering parameters (S11, S21) using established techniques such as the Nicolson–Ross–Weir (NRW) method. The resulting dielectric parameters were analyzed using the Cole–Cole relaxation model in order to extract dispersion characteristics and validate the measured data against reported literature values [1–5,7,9,10,12,21,22].

The main contribution of this work is the development of a double-layer E-comb resonator sensor that enhances electric-field confinement and improves sensitivity compared with conventional resonant sensors. The proposed sensor demonstrates a clear and selective response to polar contaminants, producing a resonance frequency shift of approximately 0.5 GHz for only 5 % (v/v) water adulteration, while showing negligible variation for sunflower oil adulteration. Furthermore, a quality factor-based purity index is introduced as a quantitative metric for assessing olive oil quality. This approach provides a rapid, non-destructive, and application-oriented sensing technique with strong potential for real-time monitoring and automated quality control in the olive oil industry, using a compact and cost-effective microwave sensing platform.

II. MATERIAL AND METHODS

A. MATERIAL AND SUBSTRATE ROLE

In the design of the proposed double-layer metamaterial sensor, FR-4 epoxy laminate was selected as the substrate material due to its wide use in microwave components, commercial availability, and cost effectiveness. The electromagnetic properties of the substrate — especially its relative permittivity and loss tangent — play a crucial role in determining the resonance behavior, field confinement, and overall sensor performance, as these parameters influence the effective electromagnetic environment around the resonator and thereby affect both the resonant frequency and quality factor.

While FR-4 provides a suitable platform for initial demonstration and validation, the use of flexible dielectric materials has been identified in the literature as a promising direction for future iterations. Flexible dielectric substrates (e.g., polymers, elastomers, and textile dielectrics) are increasingly investigated for antennas and RF sensors due to their mechanical conformability, portability, and potential integration with wearable and IoT systems, without significantly compromising dielectric performance.

These materials have been shown to exhibit low dielectric loss, mechanical flexibility, and compatibility with novel sensor designs across microwave bands.

B. SENSOR DESIGN AND SIMULATION

The proposed microwave sensor was designed as a double-layer E-comb resonator fabricated on an FR-4 epoxy substrate with relative permittivity $\varepsilon_r \approx 4.4$ and loss tangent $\tan(\delta) \approx 0.02$. The geometry and key structural parameters of the sensor are illustrated in Figure 1, with dimensions defined as follows: $a = 60\,\text{mm}$, $b = 30\,\text{mm}$, $h = 1.5\,\text{mm}$, $w = 2.5\,\text{mm}$, $g = 2\,\text{mm}$, $R = 5\,\text{mm}$, $L = 20\,\text{mm}$, and $d = 12.5\,\text{mm}$.

The E-comb resonator geometry was selected to enhance the capacitive sensing region and electric-field confinement compared with conventional single-gap resonators. The comb-type configuration introduces multiple capacitive gaps that increase fringing electric fields and improve the interaction between the resonator and the material under test (MUT). Such enhanced field localization is essential for microwave sensing applications, as the sensing mechanism relies on perturbations of the electromagnetic field caused by variations in the dielectric properties of the surrounding medium.

Full-wave electromagnetic simulations were carried out using two complementary computational techniques. The first simulation was performed using HFSS software, which employs the Finite Element Method (FEM), while the second simulation was conducted using CST Microwave Studio,

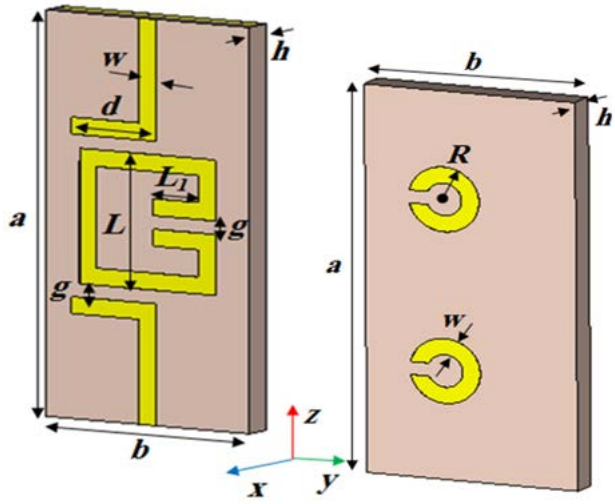

FIGURE 1. The double layer sensor schematic (E-comb resonator design).

based on the Finite Integration Technique (FIT) [23, 24]. The use of two independent electromagnetic solvers enables cross-validation of the simulated results and ensures that the predicted resonant behavior is not dependent on a particular numerical technique.

Simulations were performed for both the unloaded (empty) sensor and the sensor loaded with different liquid samples to evaluate the resonance frequency and scattering parameters (S-parameters). The resonance frequency shift observed when the sensing region is loaded with different materials forms the basis of the microwave sensing mechanism.

The rationale for adopting a metamaterial-inspired resonator structure was established through a detailed electromagnetic characterization of the corresponding metamaterial unit cell, which is presented in the following section.

C. CHARACTERIZATION OF THE METAMATERIAL SENSOR UNIT CELL

Prior to fabricating the complete sensor structure, the electromagnetic behavior of the metamaterial unit cell (Figure 2) was analyzed to evaluate its effective electromagnetic properties and verify its suitability for sensing applications.

The scattering parameters (S11, S12, S21, S22) of the unit cell were first extracted through full-wave simulations using CST Microwave Studio. These parameters were subsequently processed using MATLAB to retrieve the effective constitutive parameters, namely the effective permittivity (ε) and effective permeability (μ), as functions of frequency.

The retrieval procedure allowed the sign and dispersion characteristics of ε and μ to be analyzed across the investigated frequency band. The extracted effective parameters are plotted in Figure 3.

Figure 4 presents the standard classification of metamaterials according to the signs of the permittivity ε and the permeability μ, which defines four possible electromagnetic material categories [20,25,26]. As illustrated in Figure 3, the proposed

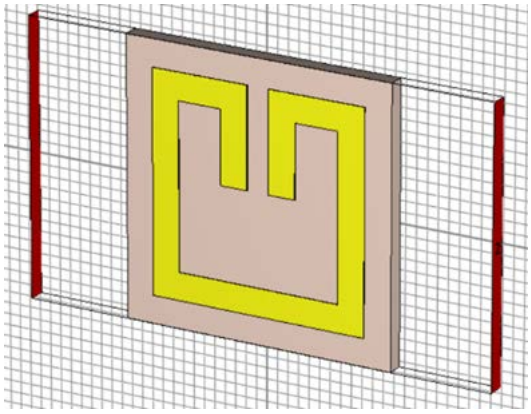

FIGURE 2. The Unit Cell of the Metamaterial.

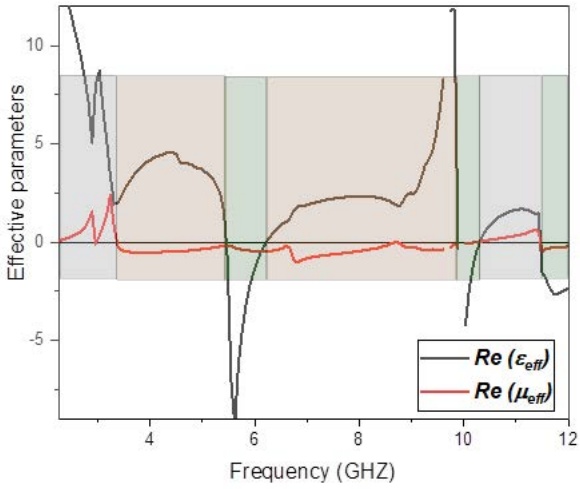

FIGURE 3. The Effective Dielectric and Magnetic Properties of the Metamaterial.

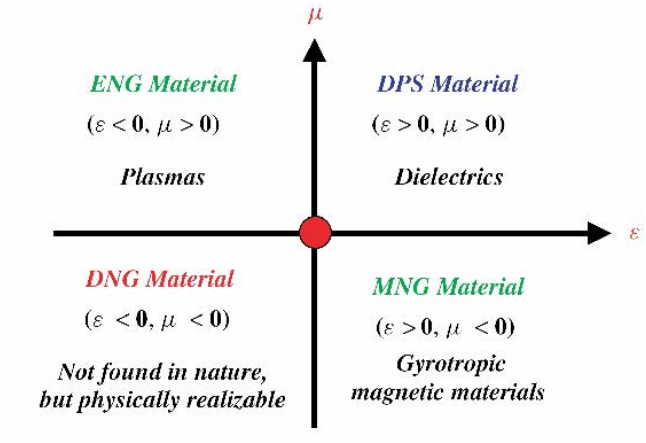

FIGURE 4. Classification of metamaterials [20,25,26].

unit cell exhibits regions of Mu-Negative (MNG) behavior, highlighted in beige, and Double-Negative (DNG) behavior,

highlighted in green.
These electromagnetic characteristics are typical of engineered metamaterials and indicate the presence of strong resonant electromagnetic interactions within the structure. The observed MNG and DNG regions span a significant portion of the investigated frequency band, which confirms that the unit cell can support resonant electromagnetic behavior over a broad spectral range.
According to established studies on metamaterial resonators [20,25,26], such broadband electromagnetic responses provide a strong foundation for wideband sensing applications, as they enable efficient interaction between the electromagnetic field and the material placed in the sensing region.

D. 2.3. SIMULATION OF ELECTRIC CURRENT DENSITY AND ELECTRIC FIELD DISTRIBUTION

To further analyze the sensing behavior of the metamaterial unit cell, the distributions of the electric current density and the electric field were simulated at the fundamental resonance frequency using CST Microwave Studio.
Figure 5 illustrates the simulated surface current density distribution, which reveals a strong concentration of induced currents along the conductive traces of the resonator. This current concentration confirms the resonant behavior of the structure and highlights the conductive paths responsible for the inductive component of the equivalent LC resonance.
Correspondingly, Figure 6 shows the electric field distribution, where a high-intensity field is clearly localized within the capacitive regions of the unit cell. This strong field confinement is particularly important for sensing applications, as it increases the interaction between the electromagnetic field and the surrounding material placed in the sensing region.
The combined analysis of current density and electric field distributions demonstrates that the proposed resonator provides strong electromagnetic field localization, which is a key indicator of a structure well suited for sensitive dielectric detection [27].

Following established modeling approaches [27,29] an equivalent circuit model was also developed for the unit cell using the magnetic wall concept. The equivalent circuit representation is illustrated in Figure 7.
In this model:

- L and C represent the distributed inductance and capacitance associated with the transmission line,
- Lr and Cr represent the inductance and capacitance of the split-ring resonator (SRR),
- The model also incorporates the magnetic coupling between the transmission line and the resonant ring.

The values of these equivalent circuit parameters were extracted using the procedures described in [30,31]. This equivalent LC model provides a physical interpretation of the resonance behavior and confirms that the sensor operates according to the classical microwave resonant sensing mechanism, where variations in the dielectric properties of the surrounding material modify the effective capacitance and consequently shift the resonance frequency.
The strong localization of the electric field in the capacitive regions of the resonator confirms the suitability of the proposed structure for microwave dielectric sensing applications.

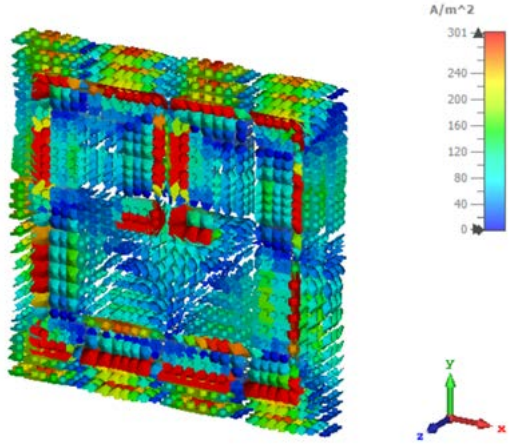

FIGURE 5. Simulation of the Electric Current Density in the unit cell using CST Software.

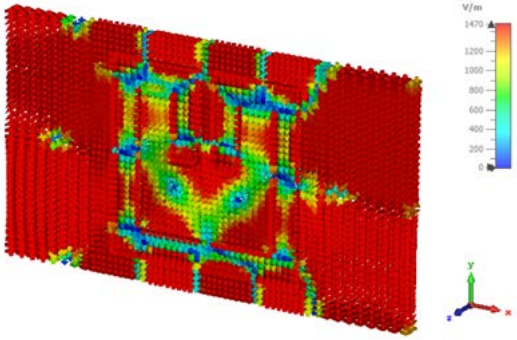

FIGURE 6. Simulation of the Electric Field in the unit cell using CST Software.

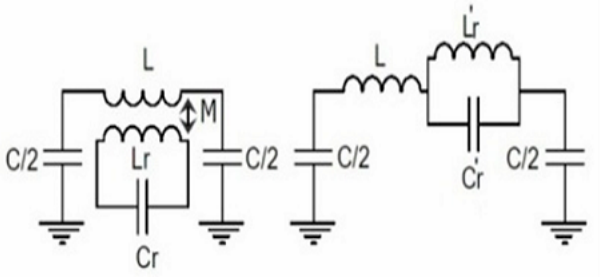

FIGURE 7. The equivalent circuit of the unit cell.

E. SENSOR FABRICATION

The sensor was fabricated as depicted in Figure 8. Its performance was characterized using an Agilent Vector Network Analyzer (VNA), calibrated via the Short-Open-Load-Thru (SOLT) method across the 1-15 GHz frequency range (see

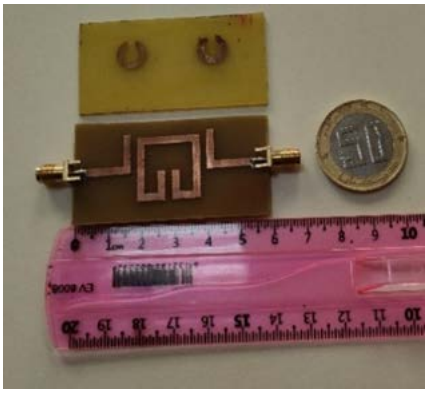

FIGURE 8. The Microwave Sensor Realization.

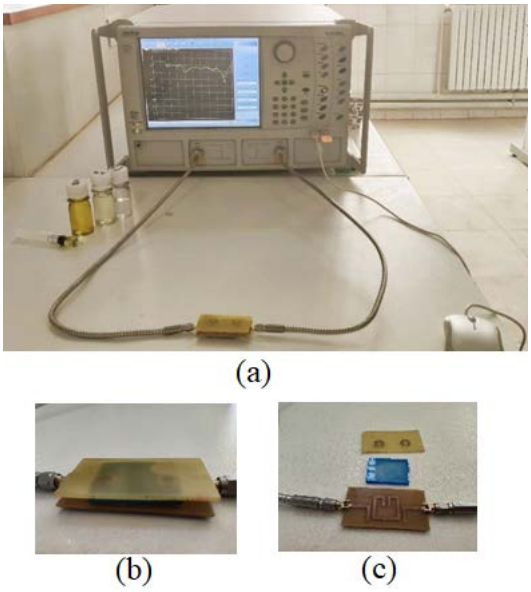

FIGURE 9. Olive oil measurements by the Microwave Sensor and the VNA.

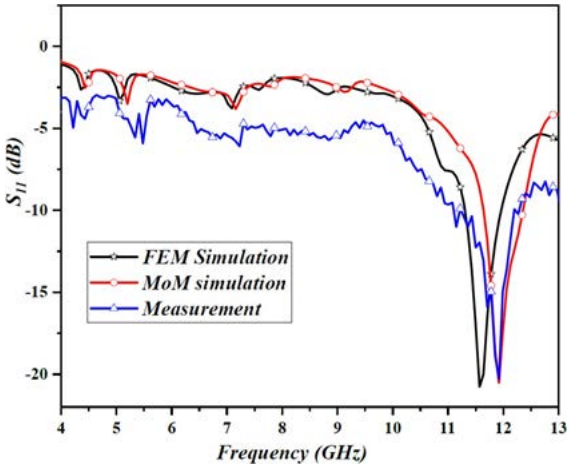

FIGURE 10. Simulated vs. experimental S11 of the empty sensor.

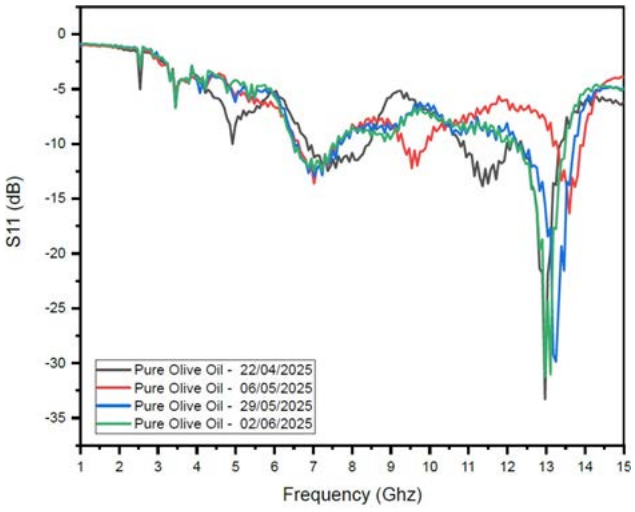

FIGURE 11. S11 measurement of pure olive oil by the sensor on different dates.

Figure 9(a)). Measurements were performed in two configurations: with and without a protective grid. The underlying sensing principle relies on the shift in the resonator's resonance frequency upon interaction with a sample. This interaction enhances electric field c onfinement wi thin the sensing region, thereby improving sensitivity, as established in the literature [13, 14, 16–18, 23, 32–38].

The proposed E-comb resonator geometry enhances the capacitive sensing region and improves electric-field localization compared with conventional SRR-based sensors.

To validate the design and fabrication accuracy, the simulated and measured reflection coefficients (S11) of the unloaded sensor are compared in Figure 10.

F. EXPERIMENTAL SETUP AND SAMPLE PREPARATION

A small rectangular container was fabricated from FR4 to ensure a consistent sample volume for all measurements. Preliminary tests confirmed the container's negligible influence on the sensor response. Its dimensions are: 35.8 mm (length) × 25.8 mm (width) × 3.15 mm (height), with a base thickness of 0.15 mm (Figure 9(c)).

Three sample types were prepared: (i) pure virgin olive oil, (ii) olive oil adulterated with 5% (v/v) water, and (iii) olive oil mixed with 5% (v/v) sunflower oil.

The 5% adulteration level was selected as it yielded a clear and reproducible shift in S-parameters, providing a robust test of the sensor's sensitivity. Measurements for each sample were conducted on multiple dates to assess repeatability (Figures 9(a), 9(b)).

G. DATA ACQUISITION AND ANALYSIS PROTOCOL

The analysis followed a sequential protocol. First, the temporal stability of the system was verified by comparing the S-parameters (S11 and S21) of pure olive oil measured on different dates (Figures 11 and 12). Subsequently, the sensor's response to adulteration was evaluated by analyzing the S-parameters for all three sample types across the measurement

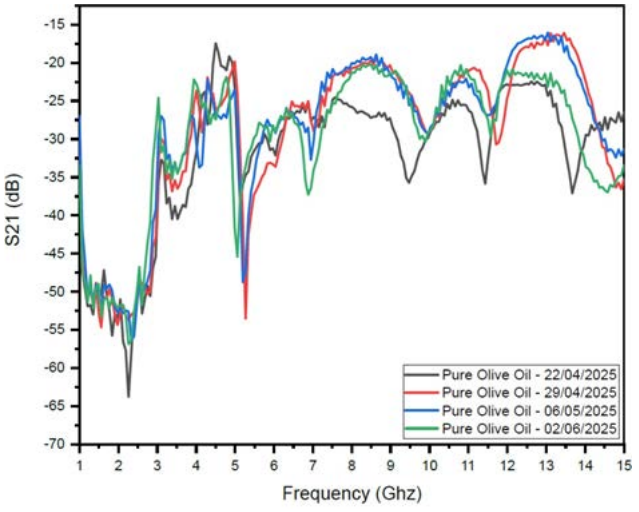

FIGURE 12. S21 measurement of pure olive oil by the sensor on different dates.

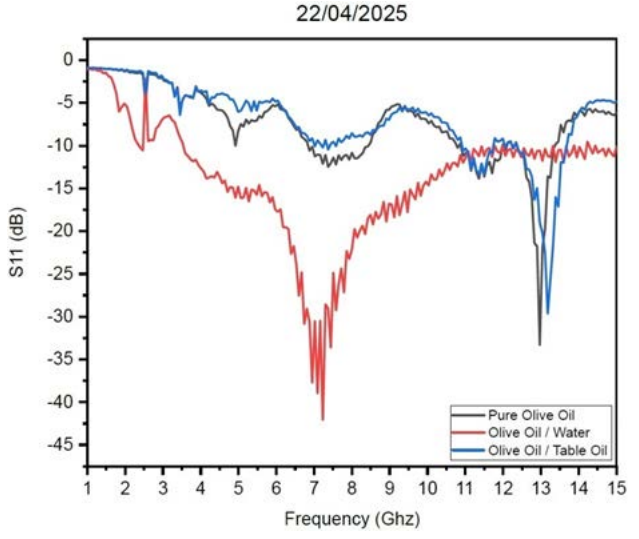

FIGURE 13. S11 measurements for pure olive oil, olive oil mixed with water, and olive oil mixed with sunflower oil, at 22/04/2025.

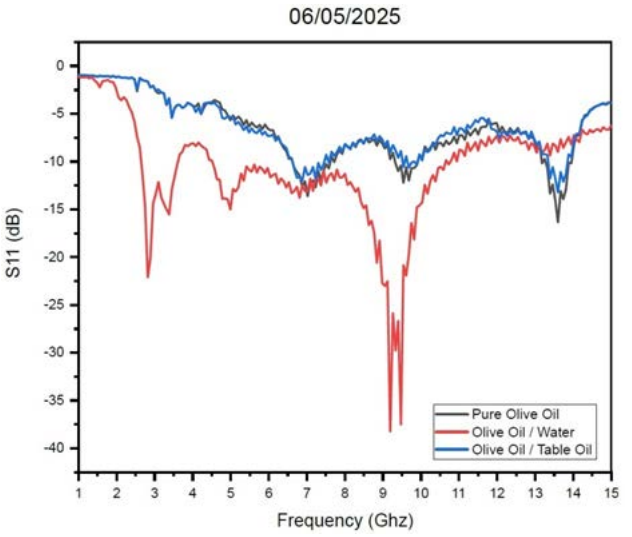

FIGURE 14. S11 measurements for pure olive oil, olive oil mixed with water, and olive oil mixed with sunflower oil, at 06/05/2025.

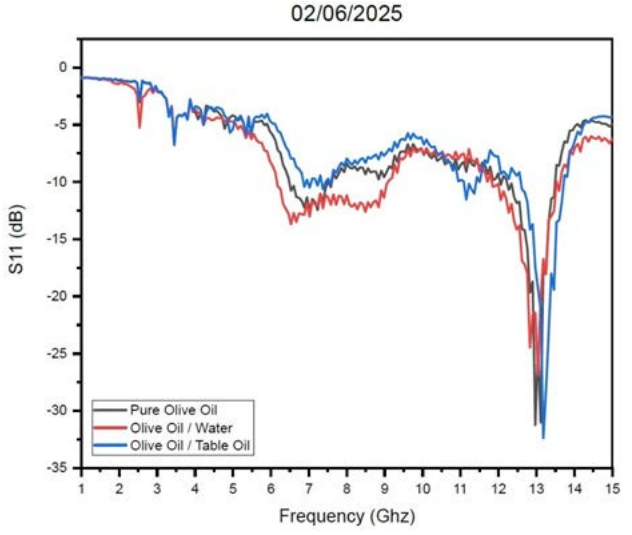

FIGURE 15. S11 measurements for pure olive oil, olive oil mixed with water, and olive oil mixed with sunflower oil, at 02/06/2025.

dates. This involved a detailed examination of the reflection coefficient (S11, Figures 13, 14, 15) and the transmission coefficient (S21, Figures 16, 17, 18).

H. DIELECTRIC MODELING AND QUALITY FACTOR

The dielectric behavior of the tested samples was analyzed through a three-stage modeling procedure.

1) The experimentally measured scattering parameters (S11 and S21) were compared with the corresponding simulation results in order to validate the electromagnetic response of the proposed sensor.
2) The complex permittivity of the samples was extracted from the measured S-parameters using the Nicolson–Ross–Weir (NRW) method, which is commonly used to determine dielectric properties from microwave measurements.
3) The extracted dielectric data were fitted using the Cole–Cole relaxation model, which describes the frequency-dependent dielectric response of polar liquids. This model allows the estimation of several key parameters, including the static permittivity (ε_s), the high-frequency permittivity (ε_∞), the relaxation time (τ), and the distribution parameter (τ), and distribution parameter (α) [1, 10, 11, 39]. The complex permittivity $\varepsilon^*(\omega)$ [1,10,11,39].

   The complex permittivity $\varepsilon^*(\omega)$ according to the Cole–Cole model is expressed as:

$$\varepsilon^*(\omega) = \varepsilon_\infty + \frac{\varepsilon_s - \varepsilon_\infty}{1 + (j\omega\tau)^{(1-\alpha')}} \quad (1)$$

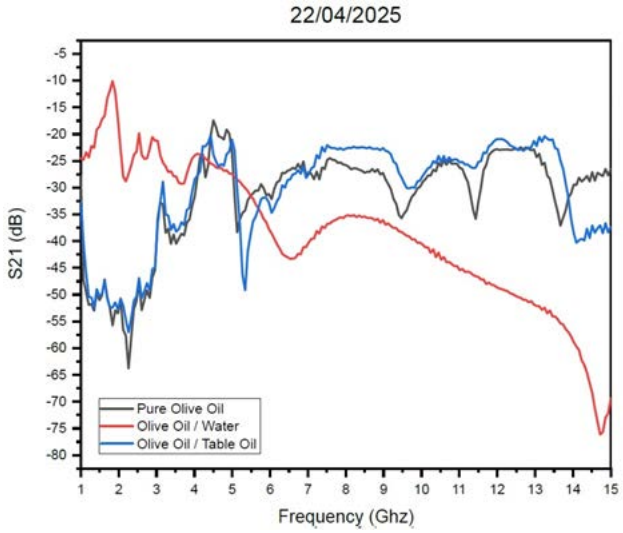

FIGURE 16. S21 measurements for pure olive oil, olive oil mixed with water, and olive oil mixed with sunflower oil, at 22/04/2025.

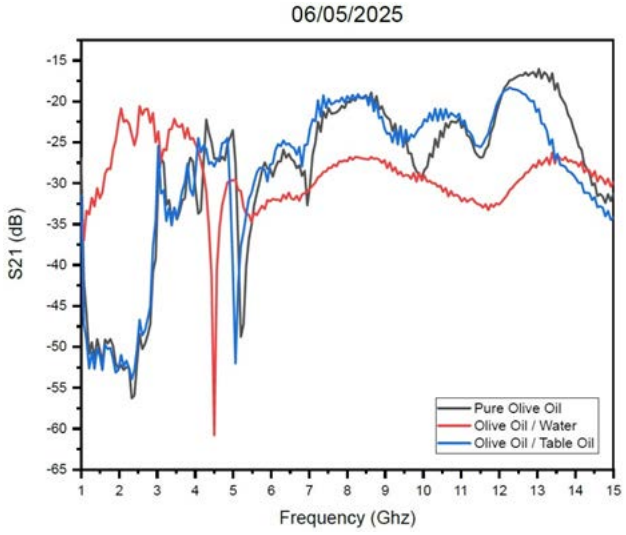

FIGURE 17. S21 measurements for pure olive oil, olive oil mixed with water, and olive oil mixed with sunflower oil, at 06/05/2025.

Where ω represents the angular frequency.

To quantitatively evaluate the sensing response of the proposed microwave sensor, a Quality Factor (QF) index was introduced as a purity indicator for olive oil samples. This index is defined as the normalized resonance frequency shift relative to the resonance frequency of pure olive oil.
The QF index is calculated as:

$$QF = \frac{|fr - fr_{\text{pure}}|}{fr_{\text{pure}}} \times 100\% \qquad (2)$$

Where fr represents the resonance frequency of the tested sample and fr_{pure} corresponds to the resonance frequency measured for pure olive oil.
This metric provides a simple and effective figure of merit for quantifying oil purity. Since water possesses a significantly higher dielectric constant than olive oil, its presence causes a substantial change in the effective permittivity surrounding the resonator, resulting in a measurable resonance frequency shift. Consequently, water-contaminated samples are expected to exhibit significantly higher QF values compared with mixtures containing non-polar oils such as sunflower oil.

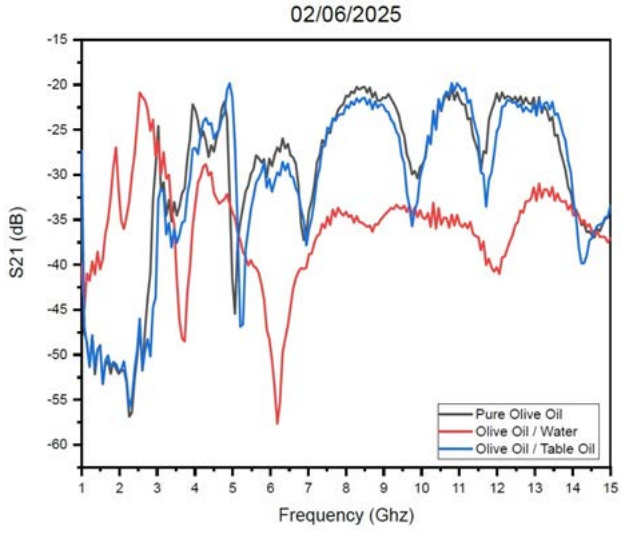

FIGURE 18. S21 measurements for pure olive oil, olive oil mixed with water, and olive oil mixed with sunflower oil, at 02/06/2025.

III. RESULTS

A. SIMULATION VS EXPERIMENTAL VALIDATION

The simulated and experimental reflection coefficient (S11) of the unloaded sensor show strong agreement, with a resonance observed near 12 GHz (Figure 10). This close correlation validates both the electromagnetic design and the fabrication fidelity of the proposed double-layer E-comb resonator structure. Minor discrepancies between simulation and measurement can be attributed to fabrication tolerances, substrate losses, and experimental uncertainties.

B. CHARACTERIZATION OF PURE OLIVE OIL

The scattering parameters (S11 and S21) measured for pure virgin olive oil, acquired on different dates, exhibit stable resonance characteristics as shown in Figures 11 and 12. The resonance frequency and amplitude remain consistent across repeated measurements, confirming both the stability of the olive oil sample and the measurement repeatability of the sensor system.
This baseline response serves as the reference state for subsequent comparisons with adulterated samples.

C. RESPONSE TO WATER ADULTERATION

The addition of 5% (v/v) water to the olive oil sample produced a pronounced resonance frequency shift of approximately 0.5 GHz, accompanied by a reduction in the minimum S11magnitude from –15 dB to –10.5 dB. At the same time,

TABLE 1. Fitted Cole-Cole parameters for the tested samples.

Sample	ϵ_s	ϵ_∞	τ (s)	α
Pure olive oil	3.71	-39.22	5.34e-01	-2.09
Olive oil+ water	0.22	-36.98	1.23e+01	-37.71
Olive oil+ Sunflower oil	2.66	-37.25	5.93e-01	-2.08

the transmission coefficient S21 exhibited increased insertion loss.

These changes indicate a strong perturbation of the electromagnetic field distribution surrounding the resonator. Since microwave resonant sensors operate by detecting variations in the effective permittivity around the sensing region, the presence of water—which has a significantly higher dielectric constant than olive oil—produces a measurable change in the resonant behavior of the structure.

D. RESPONSE TO SUNFLOWER OIL ADULTERATION

In contrast, the addition of 5% (v/v) sunflower oil resulted in only a minor resonance shift of approximately 50 MHz, with negligible change in the resonance amplitude.

This minimal response highlights the selective sensitivity of the sensor to polar contaminants such as water, while non-polar edible oils with similar dielectric properties produce only weak perturbations. The difference in response is attributed to the relatively similar dielectric constants of vegetable oils compared with the strong dielectric contrast between water and olive oil.

E. COLE-COLE PARAMETER ANALYSIS

The dielectric parameters obtained from the experimental measurements were analyzed using the Cole–Cole relaxation model, which describes the frequency-dependent dielectric response of complex liquids.

The extracted Cole–Cole parameters are summarized in Table 1. The fitting results indicate a higher static permittivity (ε_s) and broader dielectric dispersion (parameter α) for the water-contaminated sample. This behavior is consistent with the strong polar nature of water molecules and their associated dielectric relaxation mechanisms [10,11,39].

The complex permittivity obtained directly from the measured S-parameters shows excellent agreement with the Cole–Cole model across the 1–15 GHz frequency range, as illustrated in Figure 19. This agreement confirms the reliability of both the experimental measurements and the dielectric modeling approach.

F. QUALITY FACTOR ANALYSIS

A quantitative comparison of the sensor response is presented in Table 2, which summarizes the resonance frequency (F_r), frequency shift (ΔF_r), minimum S11 magnitude, and the derived Quality Factor (QF) index for each sample.

The key observations are:

- The resonance frequency of the water-adulterated sample deviates significantly from the pure olive oil reference.

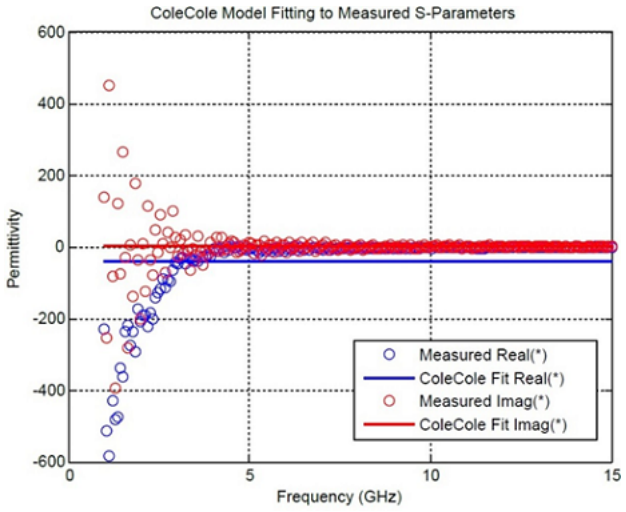

FIGURE 19. Comparison between the permittivity obtained from the measured S-parameters and the Cole-Cole model fit.

TABLE 2. Resonance frequency, quality factor index, ΔFr, and S11 min.

Sample	Fr (GHz)	ΔFr (GHz)	S11 min (dB)	QF (%)
Pure olive oil	12.00	00.00	-15.00	00.00
Olive oil+ water	11.50	-0.50	-10.50	4.17
Olive oil+ Sunflower oil	11.95	-0.05	-14.70	0.42

- The frequency shift caused by water contamination is approximately ten times greater than that produced by sunflower oil adulteration.
- The minimum S11 value becomes significantly less deep for the water-contaminated sample.
- The calculated QF index for water adulteration ($\approx 4.17\%$) is an order of magnitude larger than that for sunflower oil ($\approx 0.42\%$).

These results confirm that water produces a distinct dielectric signature compared with other edible oils [3,4,6,40]. The QF index therefore provides a simple and effective quantitative indicator for detecting water contamination in olive oil.

IV. DISCUSSION

This study demonstrates the reliable detection of water adulteration in virgin olive oil using a double-layer metamaterial microwave sensor. The proposed sensor exhibited a pronounced and selective response to the polar water contaminant, manifested as a significant resonance frequency shift of approximately 0.5 GHz for 5% water adulteration, accompanied by changes in the S-parameter magnitude.

Dielectric modeling using the Cole–Cole relaxation model further corroborated these experimental observations, quantitatively confirming the large dielectric contrast between olive oil and water.

The obtained results are consistent with previous studies investigating the dielectric properties of edible oils and the use of metamaterial-based sensors for food quality monitor-

TABLE 3. Proposed Double-Layer Metamaterial Sensor vs. Recent Work.

Reference	Sensor Structure	Application	Validation Method	Operating Frequency	Frequency Shift / Sensitivity	Quality Factor (QF)	Key Characteristics
This study	Double-layer metamaterial sensor based on E-comb resonator patterned on FR-4 substrate	Detection of 5% water adulteration in olive oil	Full-wave simulation (CST, HFSS) and experimental validation (VNA)	1–15 GHz	0.5 GHz resonance shift	4.17	Double-layer microwave resonator enabling automatic detection of water adulteration in virgin olive oil
Huang et al. (2019) [43]	Metamaterial absorber sensor	Detection of water content in emulsified oil	Simulation and experiment	10–11 GHz	339 MHz/ϵ_r sensitivity	Not reported	Demonstrates linear resonance shift with dielectric constant variation
Bhatti et al. (2022) [44]	CSRR microwave resonator	Detection of adulteration in edible oils	Simulation and experiment	5.25 GHz	530 MHz maximum frequency shift	39	Low-cost compact FR-4 sensor for edible oil characterization
Islam et al. (2022) [45]	Rectangular enclosed metamaterial sensor	Multi-liquid identification including olive oil	Simulation and experiment	Not specified	Not reported	~ 135	Strong microwave interaction with liquid samples
Star SRR sensor, Islam et al (2023) [46]	Star-enclosed circular split-ring resonator metamaterial	Differentiation among various liquids and oils	Simulation	X-band	$\sim$ 410 MHz shift	~ 430	High-Q resonator enabling multi-liquid discrimination
Qureshi et al (2021) [47]	G-shaped metamaterial absorber	Detection of different edible oils	Simulation and experiment	X-band	$\sim$ 180 MHz shift	Not reported	Oil identification based on resonance variation
Dhingra et al (2025) [48]	Microwave-aided sensor two square-shaped resonators	Adulteration-mustatd-oil	Simulation and experiment	1 -5 GHz	Sensitivity of 0.1	Not reported	Assessment of the dielectric characteristic of adulterated oil samples of mustard
Korkamaz and Hasar (2024) [49]	Microwave engraved split-ring resonator	Detection of olive oil adulteration with sunflower oil	Simulation and experiment	2–9 GHz	$\sim$ 62 MHz shift	Not reported	CSRR-based microwave structure for oil quality monitoring
Musa Hussain et al (2023)[50]	Compact metamaterial liquid sensor	Quality monitoring of oils and fuels	Simulation CST	X-band 8–12GHz	Sensitivity $\approx$ 0.91	~ 350	Compact metamaterial design with high sensing performancesuitable for radar and military applications

ing [1,3,8,9,13,14,33,34,39–42]. Importantly, the proposed sensor was able to produce a clear measurable response at a relatively low adulteration level of 5% (v/v), highlighting its practical sensitivity.

The Quality Factor (QF) index introduced in this work provides a convenient quantitative metric for oil purity evaluation. By transforming the complex electromagnetic response into a simple numerical indicator, the QF index enables rapid assessment of oil quality and facilitates real-time monitoring. Following calibration using a pure reference sample, the proposed sensor could potentially be integrated into industrial environments, such as storage tanks or filling pipelines, enabling continuous and automated quality control in olive oil production systems.

To further position the proposed sensor within the existing literature, Table 3 summarizes representative microwave and metamaterial sensors reported for liquid and oil characterization.

V. COMPARATIVE DISCUSSION

The proposed double-layer metamaterial sensor based on an E-comb resonator patterned on an FR-4 substrate demonstrates strong sensitivity to dielectric perturbations caused by water contamination in olive oil.

The sensor operates over a broad frequency range (1–15 GHz) and exhibits a measurable resonance shift of 0.5 GHz for only 5% water adulteration, with a calculated Q-factor index of approximately 4.17.

When compared with previously reported microwave resonant sensors, several observations can be made. For instance, CSRR-based microwave sensors fabricated on FR-4 substrates have been used to detect edible oil adulteration with frequency shifts up to 530 MHz and quality factors around 39. Other metamaterial-based sensors operating in the X-band (8–12 GHz) have demonstrated Q-factors up to 350 for liquid characterization.

While some reported sensors exhibit higher Q-factors, they often operate over narrower frequency bands or require more complex resonator geometries. In contrast, the proposed sen-

sor provides broadband operation, simple planar fabrication, and reliable detection of low-level water adulteration.

These characteristics highlight the practical applicability of the proposed sensor for non-destructive liquid quality monitoring using a compact and cost-effective microwave sensing platform.

VI. CONCLUSION

This work presented a double-layer metamaterial microwave sensor based on an E-comb resonator for detecting water adulteration in virgin olive oil.

The proposed sensor was designed, simulated using full-wave electromagnetic methods (HFSS and CST), fabricated, and experimentally validated using vector network analyzer measurements across the 1–15 GHz frequency range.

The proposed E-comb resonator geometry enhances the capacitive sensing region and improves electric-field localization compared with conventional SRR-based sensors.

The experimental results demonstrate that the sensor exhibits high selectivity and sensitivity to water contamination, producing a measurable resonance frequency shift of approximately 0.5 GHz for only 5% (v/v) water adulteration, while showing negligible response to sunflower oil adulteration.

Dielectric characterization using the Cole–Cole model confirmed that the extracted dielectric properties are consistent with reported literature values. In addition, the proposed QF-based purity index enables rapid and quantitative evaluation of oil quality.

Overall, the results highlight the strong potential of the proposed sensing approach for non-destructive, real-time monitoring of olive oil quality, using a compact and cost-effective microwave sensing platform.

Future work will focus on improving the detection limit, optimizing the resonator geometry, the use of flexible dielectric materials, or microfluidic antenna, and extending the sensing approach to other edible oils and liquid food products.

REFERENCES

[1] N. Segatin, T. Pajk Zontar, and N. Poklar Ulrih. Dielectric properties and dipole moment of edible oils subjected to “frying” thermal treatment. Foods, 9(7):900, 2020, (doi: 10.3390/foods9070900).

[2] J. Vrba and D. Vrba. "Temperature and frequency dependent empirical models of dielectric properties of sunflower and olive oil". Radioengineering, 22(4):1281–1287, Dec 2013. https://www.radioeng.cz/fulltexts/2013/13_04_1281_1287.pdf.

[3] L. Hu, K. Toyoda, and I. Ihara. Dielectric properties of edible oils and fatty acids as a function of frequency, temperature, moisture and composition. Journal of Food Engineering, 88(2):151–158, 2008, (doi: 10.1016/j.jfoodeng.2007.12.035).

[4] S. E. Drici and A. Drici. "Etude de qualité de l’huile d’olive algérienne : effet des conditions de stockage". Master’s thesis, Université 8 Mai 1945, Guelma, 2019. https://dspace.univ-guelma.dz/jspui/handle/123456789/4566.

[5] I. Ben Tekaya and M. Hassouna. "Etude de la stabilité oxydative de l’huile d’olive vierge extra tunisienne au cours de son stockage". OCL, 12(5–6), 2005. https://www.ocl-journal.org/articles/ocl/pdf/2005/05/ocl2005125-6p447.pdf.

[6] S. Ait Habib and A. Ouikene. "Etude de quelques caractéristiques physico-chimiques de l’huile d’olive de la variété chemlal de la région de maatkas (tizi-ouzou)". Master’s thesis, Université Mouloud Mammeri, 2017. https://dspace.ummto.dz/server/api/core/bitstreams/d2e46ff9-b635-4291-a19f-1d6ef3b79f7f/content.

[7] N. F. Attafi, I. Bouramssa, B. Labreche, and F. Mouhallel. "Contribu-tion à l’étude de la qualité d’huile d’olive de trois régions : Guelma, skikda et jijel". Master’s thesis, Université 8 Mai 1945, Guelma, 2022. http://dspace.univ-guelma.dz/jspui/handle/123456789/13831.

[8] M. Djillali Benayed. "Etude physico-chimique de l’huile d’olive". Master’s thesis, Agroalimentaire – Contrôle de Qualité, 2020. https://dspace.univ-temouchent.edu.dz/server/api/core/bitstreams/3b3e875e-b59e-4a20-9da1-56a792836548/content.

[9] H. Banting and C. E. Saavedra. Dielectric spectroscopy of fluids and polymers for microwave microfluidic circuits and antennas. IEEE Transactions on Microwave Theory and Techniques, 69(1):337–343, Jan 2021, (doi: 10.1109/TMTT.2020.3020627).

[10] W. Ellison. Permittivity of pure water over the frequency range 0–25 thz and the temperature range 0–100∞c. Journal of Physical and Chemical Reference Data, 36(1):1–18, 2007, doi: 10.1063/1.2360986).

[11] K. S. Cole and R. H. Cole. Dispersion and absorption in dielectrics i. alternating current characteristics. The Journal of Chemical Physics, 9:341–351, 1941, (doi: 10.1063/1.1750906).

[12] J. Corach, P. A. Sorichetti, and S. D. Romano. Electrical properties of vegetable oils between 20 hz and 2 mhz. International Journal of Hydrogen Energy, 39(16):8754–8758, 2014, (doi: 10.1016/j.ijhydene.2013.12.036).

[13] V. Naresh and N. Lee. A review on biosensors and recent developments of nanostructured materials-enabled biosensors. Sensors, 21(4):1109, 2021, (doi: 10.3390/s21041109).

[14] X. Han, Y. Zhou, X. Li, Z. Ma, L. Qiao, C. Fu, and P. Peng. Microfluidic microwave sensor loaded with star-slotted patch for edible oil quality inspection. Sensors, 22(17):6410, 2022, (doi: 10.3390/s22176410).

[15] A. Valipour, M. H. Kargozarfard, M. Rakhshi, A. Yaghootian, and H. M. Sedighi. Metamaterials and their applications: An overview. Proceedings of the Institution of Mechanical Engineers, Part L: Journal of Materials: Design and Applications, 236:2171–2210, 2022, (doi: 10.1177/1464420721995858).

[16] V. Kaushik. Metamaterials, Apr 2019, (doi: 10.13140/RG.2.2.28478.64322).

[17] W. J. Padilla, D. N. Basov, and D. R. Smith. Negative refractive index metamaterials. Materials Today, 9(7–8):28–35, Jul 2006, (doi: 10.1016/S1369-7021(06)71573-5).

[18] A. Arjunan, A. Baroutaji, J. Robinson, A. Vance, and A. Arafat. Acoustic metamaterials for sound absorption and insulation in buildings. Building and Environment, 251:111250, 2024, (doi: 10.1016/j.buildenv.2024.111250).

[19] H. Al Ajmi, M. Bait-Suwailam, and M. Masoud. Efficiency enhancement of photovoltaic solar cells using metamaterials absorbing screen. Journal of Engineering Research, 19(2):85–94, 2022, (doi: 10.53540/tjer.vol19iss2pp85-94).

[20] Gurwinder Singh et al. A review of metamaterials and its applications. International Journal of Engineering Trends and Technology, 19(6):305–310, 2015, (doi: 10.14445/22315381/IJETT-V19P254).

[21] M. A. Ben Aissa. "Etude de la stabilité oxydative de l’huile d’olive vierge extra tunisienne". Doctoral thesis, Université de Sfax, 2020.

[22] C. Tran Duy. "Propriétés diélectriques de liquides isolants d’origine végétale pour applications en haute tension". Ph.d. dissertation, Université Joseph Fourier, 2009. https://theses.hal.science/tel-00827638v1.

[23] S. Mosbah. "Modélisation et réalisation d’un capteur micro-onde à base de métamaterials". Ph.d. dissertation, Université Ferhat Abbas, Sétif 1, 2023. http://dspace.univ-setif.dz:8888/jspui/handle/123456789/4054.

[24] Kang Luo, Song-Hu Ge, Lei Zhang, Hong-Bo Liu, and Jin-Ling Xing. Simulation analysis of ansys hfss and cst microwave studio for frequency selective surface. In 2019 International Conference on Microwave and Millimeter Wave Technology (ICMMT), pages 1–3. IEEE, 2019, (doi: 10.1109/ICMMT45702.2019.8992280).

[25] Ms. Vandana Kaushik. Negative index materials: Metamaterials. Research Review International Journal of Multidisciplinary, 4(4), April 2019. https://old.rrjournals.com/wp-content/uploads/2019/04/664-669_RRIJM190404142.pdf.

[26] M. Hussain, et al. Metamaterials and Their Application in the Performance Enhancement of Reconfigurable Antennas: A Review. Micromachines MDPI, 14:3491, 2023, (doi: 10.3390/mi14020349).

[27] Nourelhouda Dadouche, Zinelabiddine Mezache, et al. Design and fabrication of a novel corona-shaped metamaterial biosensor for cancer cell detection. Micromachines, 14(11):2114, 2023, (doi: 10.3390/mi14112114).

[28] Bahareh Moradi, Raul Fernandez-Garcıa, and Ignacio Gil. E-textile embroidered metamaterial transmission line for signal propagation control. Materials, 11(6):955, 2018, (doi: 10.3390/ma11060955).

[29] Juan Domingo Baena, Jordi Bonache, Ferran Martın, et al. Equivalent-circuit models for split-ring resonators and complementary split-ring resonators coupled to planar transmission lines. IEEE Transactions on Microwave Theory and Techniques, 53(4):1451–1461, 2005, (doi: 10.1109/TMTT.2005.845211).

[30] Jia-Shen G. Hong and Michael J. Lancaster. "Microstrip Filters for RF/Microwave Applications". John Wiley & Sons, 2004. https://download.e-bookshelf.de/download/0000/5819/00/L-G-0000581901-0002360393.pdf.

[31] Yadgar I. Abdulkarim, Lianwen Deng, Muharrem Karaaslan, et al. Novel metamaterials-based hypersensitized liquid sensor integrating omega-shaped resonator with microstrip transmission line. Sensors, 20(3):943, 2020, (doi: 10.3390/s20030943).

[32] Ansoft Corporation. "Electronic Design Automation Software User's Guide – High Frequency Structure Simulator" 10, 2005. https://saaubi.people.wm.edu/ResearchGroup/Docs/HFSSv10UserGuide.pdf.

[33] O. Malyuskin. Microplastic detection in soil and water using resonance microwave spectroscopy: A feasibility study. IEEE Sensors Journal, 20(24):14817–14826, 2020, (doi: 10.1109/JSEN.2020.3011311).

[34] Y. S. Cho and S.-J. Gwak. Novel sensing technique for stem cell differentiation using dielectric spectroscopy of their proteins. Sensors, 23(5):2397, 2023, (doi: 10.3390/s23052397).

[35] Javalkar Vinay Kumar, N. Shylashree, Seema Srinivas, Ajit Khosla, C. Manjunatha, et al. Review on biosensors: Fundamentals, classifications, characteristics, simulations, and potential applications. ECS Transactions, 107(1):13005, 2022, (doi: 10.1149/10701.13005ecst).

[36] D. Belmessaoud. "Etude de nouvelles antennes planaires en tenant compte des surfaces sélectives en fréquence". Doctoral thesis, Université Mohamed Boudiaf – M'sila, 2020. https://theses-algerie.com/2962280283237017/these-de-doctorat/universite-mohamed-boudiaf—m-sila/etude-de-nouvelles-antennes-planaires-en-tenant-compte-des-surfaces-selectives-en-frequence.

[37] K. Jaruwongrungsee et al. Microfluidic-based split-ring-resonator sensor for real-time and label-free biosensing. In Procedia Engineering, volume 120, pages 163–166, 2015, (doi: 10.1016/j.proeng.2015.08.595).

[38] N. Alrayes and M. I. Hussein. Metamaterial-based sensor design using split ring resonator and hilbert fractal for biomedical applications. Sensing and Bio-Sensing Research, 31:100395, 2021, (doi: 10.1016/j.sbsr.2020.100395).

[39] G. V. Umoh, J. E. Leal-Perez, S. F. Olive-Mendez, et al. Complex dielectric function, cole–cole, and optical properties evaluation in bimno3 thin films by veels analysis. Ceramics International, 48:22141–22146, 2022, (doi: 10.1016/j.ceramint.2022.04.212).

[40] M. A. Baqir, et al. Large quality factor metasurface-based biosensor for glucose monitoring. Journal of the Optical Society of America B, 42(7):1651–1655, Jul 2025, (doi: 10.1364/JOSAB.559129).

[41] X. Huang, et al. Highly sensitive biosensor based on metamaterial absorber with an all-metal structure. IEEE Sensors Journal, 23(4):3573–3580, Feb 2023, (doi: 10.1109/JSEN.2023.3235897).

[42] Bilal Tutuncu. Metamaterial biosensor for ism band biomedical applications. In 2020 4th International Symposium on Multidisciplinary Studies and Innovative Technologies (ISMSIT), Istanbul, Turkey, Oct 2020. IEEE, (doi: 10.1109/ISMSIT50672.2020.9255114).

[43] J. Huang, et al. Detection of Water Content in Emulsified Oil with the Metamaterial Sensor. Progress In Electromagnetics Research M, 85:135-144, 2019 (doi: 10.2528/PIERM19063002).

[44] M. H. Bhati, et al. Low-Cost Microwave Sensor for Characterization and Adulteration Detection in Edible Oil. Applied Sciences MDPI, 12(17):8665, 2022, (doi: 10.3390/app12178665).

[45] M. R. Islam, et al. Metamaterial sensor based on rectangular enclosed adjacent triple circle split ring resonator with good quality factor for microwave sensing application. Scientific Reports, 12:6792, 2022, (doi: 10.1038/s41598-022-10729-4).

[46] M. R. Islam, et al. Star enclosed circle split ring resonator-based metamaterial sensor for fuel and oil adulteration detection. Alexandria Engineering Journal, 67:547-563, 2023, (doi: 10.1016/j.aej.2023.01.001).

[47] S. A. Qureshi, et al. Millimetre-Wave Metamaterial-Based Sensor for Characterisation of Cooking Oils. International Journal of Antennas and Propagation, 5520268:10p3, 2021, (doi: 10.1155/2021/5520268).

[48] N. Dhingra and N. Saluja. Application of Radio Frequency Microwave Sensors to Identify Adulteration in Mustard Oil. Food Analytical Methods, 18:963–972, 2025, (doi: 10.1007/s12161-025-02766-2).

[49] H. Korkamaz and U.C. Hazar. Sensitive Microwave Sensor for Adulteration Detection in Olive Oil. Natural Sciences and Engineering Bulletin, 1(2):27-37, 2024, (https://izlik.org/JA64ZL82FU).

[50] M. Hussain, et al. Miniature Broadband Electromagnetic Wave Absorber for X-band Signals. in: 2023 XXXVth General Assembly and Scientific Symposium of the International Union of Radio Science (URSI GASS), 19-26 August 2023, (doi: 10.23919/URSIGASS57860.2023.10265613).